Comparative Medicine
Copyright 2014
by the American Association for Laboratory Animal Science

Vol 64, No 1
February 2014
Pages 34–43

Original Research

Spontaneous Intraocular Hemorrhage in Rats during Postnatal Ocular Development

Katsuhiro Inagaki,[1,2,*] Hiroyasu Koga,[1] Kazuyoshi Inoue,[1] Katsushi Suzuki,[2] and Hiroetsu Suzuki[2]

To study spontaneous intraocular hemorrhage in rats during postnatal ocular development and to elucidate the underlying mechanism, postnatal ocular development in the albino Wistar Hannover (WH) and Sprague–Dawley (SpD) and pigmented Long–Evans (LE) strains was analyzed. Pups (*n* = 2 to 5) from each strain were euthanized daily on postnatal days (PND) 0 through 21 and their eyes examined macroscopically and histologically; similar analyses were performed in 26 to 39 additional WH pups daily from PND 7 to 14. At necropsy, ring-shaped red regions and red spots were present in the eyes of WH and SpD rats. These lesions were attributed histologically to hemorrhage of the tunica vasculosa lentis or of the retina, choroid, and hyaloid artery, respectively. Similar intraocular hemorrhages occurred in LE rats, although the macroscopic alterations found in WH and SpD rats were not present in this strain. Among the 3 strains evaluated, the incidence of the intraocular hemorrhage was highest in WH rats. We here showed that intraocular hemorrhage occurs spontaneously during normal ocular development in rats regardless of the strain; however, the region, degree, and incidence of intraocular hemorrhage differ among strains. Hemorrhage in the tunica vasculosa lentis and hyaloid artery may result from the leakage of erythrocytes from the temporary vasculature of these tissues during regression. The mechanisms underlying hemorrhage in the retina and choroid remain unclear. To our knowledge, this report is the first to describe the spontaneous intraocular hemorrhage that occurs during postnatal ocular development in rats.

Abbreviations: LE, Long–Evans; PND, postnatal day; SpD, Sprague–Dawley; WH, Wistar Hannover.

Typically rats are used in reproductive toxicity studies. Until recently, Sprague–Dawley (SpD) rats have been the default test strain for such studies. However, in 2006, an albino strain of Wistar Hannover (WH) rat was newly recommended as a test strain for toxicologic studies, including reproductive toxicity studies, by the National Toxicology Program.[9] To obtain historical control data from WH rats for reproductive toxicity studies, we performed a preliminary examination of various developmental indices of pups, including parameters such as viability, body weight, sexual maturation, sex ratio, and organ histogenesis. During this examination, we collected samples from lactating rats, weanlings, culled pups, and accidental deaths. We subsequently encountered ring-shaped red regions and red spots in the eyeballs of pups before eye opening. At the time, we speculated that these ocular alterations resulted from intraocular hemorrhage. We had previously never noted intraocular hemorrhage in SpD pups, although we did not regularly examine the eyes before eye opening as part of the standard testing protocol for reproductive toxicity studies.[17] In addition, we could not locate any report that described intraocular hemorrhage in rat pups before eye opening. Therefore, we needed to confirm whether this early-postnatal intraocular hemorrhage occurs specifically in WH rats and to elucidate its mechanism. Here we describe our detailed, comparative pathologic analysis of postnatal ocular development in albino WH and SpD and pigmented Long–Evans (LE) rats.

Received: 16 May 2013. Revision requested: 26 Jun 2013. Accepted: 01 Aug 2013.
[1]Research Center, Nihon Nohyaku, Kawachi-Nagano, Osaka, Japan; [2]Laboratory of Veterinary Physiology, Nippon Veterinary and Life Science University, Musashino-shi, Tokyo, Japan
[*]Corresponding author. Email: inagaki-katsuhiro@nichino.co.jp

Materials and Methods

Animals. WH ([BrlHan:WIST@Jcl [GALAS]) and SpD (Crl:CD) rats were purchased from CLEA Japan (Tokyo, Japan) and Charles River Laboratories Japan (Kanagawa, Japan), respectively. LE (Iar:Long–Evans) rats were purchased from the Institute for Animal Reproduction (Ibaraki, Japan). The animals obtained were SPF pregnant female rats at gestational days 14 to 16 and were acclimated to our laboratory conditions for more than 5 d, which included a quarantine period. Rats were housed individually in polycarbonate cages throughout the experimental period in a room maintained at a temperature of 22 ± 3 °C, a relative humidity of 50 ± 20%, a ventilation recirculation rate of 12 to 15 complete fresh-air changes hourly, and a 12:12-h light:dark cycle. The rats were given access to a pelletized diet (MF, Oriental Yeast, Tokyo, Japan) and tap water ad libitum. The health status of the pregnant dams was monitored daily, and they were allowed to deliver. Randomly selected offspring from each litter were used for the study.

Animal care and use conformed to the standards established by the animal welfare committee of the institute and complied with all legal requirements for the humane treatment and management of animals.[15]

Outline of experiments. ***Experiment 1.*** The incidences of ring-shaped red regions and red spots in the eyes and any associated

Table 1. The incidences of macroscopic ocular lesions at necropsy in the pups of 3 rat strains at PND 0-21

Strain		PND 0	1	2	3	4	5	6	7	8	9	10	11	12	13	14	15	16	17	18	19	20	21	Cumulative incidence
WH																								
	Total no. of pups examined	2	3	3	3	2	3	3	3	3	3	2	2	2	2	2	2	2	3	3	2	2	2	54
	No. of pups with any macroscopic findings	0	0	0	0	0	0	0	0	2	2	2	2	2	1	2	1	1	0	0	1	0	0	16 (29.6)[a]
	No. of pups with ring-shaped red region in anterior segment	0	0	0	0	0	0	0	0	0	1	2	2	2	1	1	1	0	0	0	0	0	0	10 (18.5)[d]
	No. of pups with red spot in posterior segment	0	0	0	0	0	0	0	0	2	1	**2**	0	**1**	**1**	1	0	1	0	0	1	0	0	10 (18.5)[g]
SpD																								
	Total no. of pups examined	4	4	4	4	4	4	4	5	4	5	5	5	5	5	5	4	4	4	4	4	4	4	95
	No. of pups with any macroscopic findings	0	0	0	1	0	0	0	0	0	4	1	1	1	0	1	0	0	0	0	0	0	0	9 (9.5)[b]
	No. of pups with ring-shaped red region in anterior segment	0	0	0	1	0	0	0	0	0	4	1	1	0	0	0	0	0	0	0	0	0	0	7 (7.4)[e]
	No. of pups with red spot in posterior segment	0	0	0	0	0	0	0	0	0	**1**	0	0	1	0	1	0	0	0	0	0	0	0	3 (3.2)[h]
LE																								
	Total no. of pups examined	4	4	4	4	4	4	4	4	3	4	4	4	4	4	4	4	4	4	4	4	4	4	87
	No. of pups with any macroscopic findings	0	0	0	0	0	0	0	0	0	0	0	0	0	0	0	0	0	0	0	0	0	0	0 (0.0)[c]
	No. of pups with ring-shaped red region in anterior segment	0	0	0	0	0	0	0	0	0	0	0	0	0	0	0	0	0	0	0	0	0	0	0 (0.0)[f]
	No. of pups with red spot in posterior segment	0	0	0	0	0	0	0	0	0	0	0	0	0	0	0	0	0	0	0	0	0	0	0 (0.0)[h]

The values in parentheses indicate the cumulative incidence as a percentage. Bold type indicates simultaneous occurrence with ring-shaped red regions.

[a, b, c]These values differ significantly ($P < 0.05$, one-tailed Fisher exact test).

[d, e, f]These values differ significantly ($P < 0.05$, one-tailed Fisher exact test).

[g, h]These values differ significantly ($P < 0.05$, one-tailed Fisher exact test).

histopathologic findings were compared among the 3 rat strains. Six WH dams, 7 SpD dams, and 7 LE dams were used. Two to 5 pups born to the dams of each strain were selected randomly and euthanized daily from PND 0 (the day of birth) through 21. The pups were euthanized by exsanguination from the abdominal aorta under ether anesthesia, and the eyes were excised for macroscopic and histopathologic evaluation.

Experiment 2. A detailed study was performed by using WH rats, because this strain demonstrated the highest incidence of ocular alterations in experiment 1. Thirty WH additional pregnant dams were used; 26 to 39 pups born to 3 or 4 dams were euthanized daily from PND 7 through 14 as described for experiment 1, and the eyes were excised.

Macroscopic observation of eyes and measurement of eye volume. The eyes of pups were assessed macroscopically daily after birth. The day of eye opening, defined as complete opening of both eyelids, was recorded. At necropsy, the excised eyes were evaluated grossly, and the incidences of ring-shaped red regions and red spots were recorded. The width and depth of the eyes were measured by using a vernier caliper, and the volume of the eyeball was calculated as an ellipsoid by using the following formula:

$$\text{Volume of eye (mm}^3\text{)} = 4 \times 3.14 \times (\text{width [mm]} / 2)^2 \times (\text{depth [mm]} / 2) / 3$$

The mean eye volume was calculated for each pup and was considered to be a representative value of the volume of each eye in that animal.

Histopathologic examination of eyes. Eyes were prefixed overnight in a freshly prepared solution containing 1.4% (v/v) glutaraldehyde, 1.5% (v/v) formalin, and 1% (v/v) acetic acid in 0.07 M phosphate buffer (pH 7.2) and then fixed in 10% buffered formalin (pH 7.2) for more than 1 wk.[6] The eye with greater macroscopic alteration was selected from each pup as a representative sample for histopathology. The selected eyes were em-

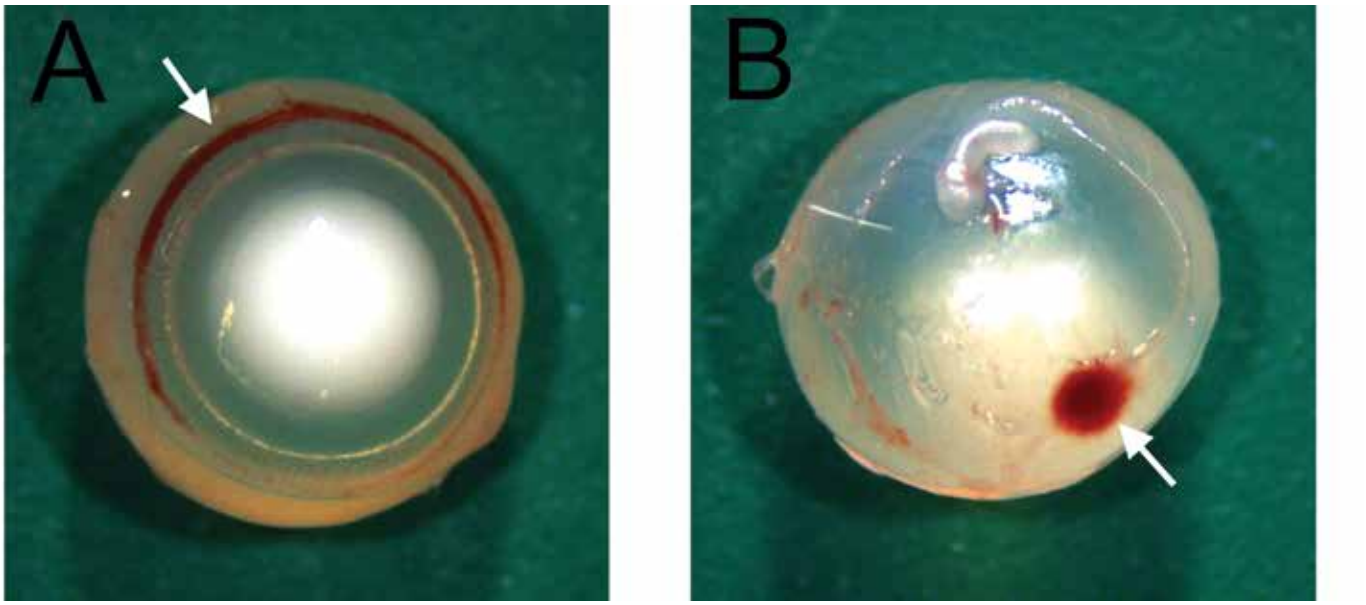

Figure 1. Abnormal eyes from pups born to normal WH dams. (A) A ring-shaped red region (arrow) in the anterior ocular segment (frontal view). (B) A red spot (arrow) in the posterior ocular segment (posterior view).

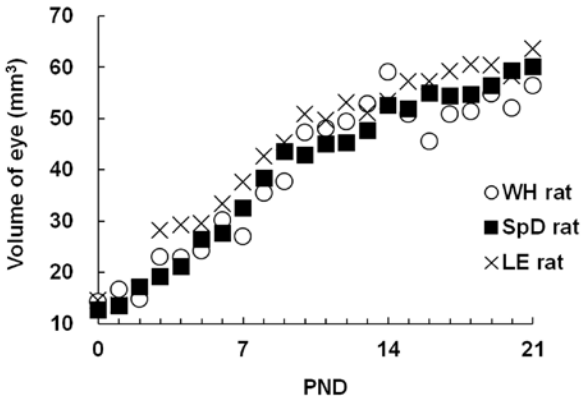

Figure 2. Age-related changes in eye volume during PND 0 through 21 in pups from 3 rat strains. The values represent the average of 2 to 5 pups.

bedded in paraffin and sagittally sectioned (1 µm) according to routine methodology. To identify the origin of the erythrocytes in the trabecular meshwork and aqueous chamber, serial sections of representative eyes from WH rats at PND 7 through 14 were also prepared. The sections were stained with hematoxylin and eosin for light microscopy, but some parts of the sections were stained with Martius scarlet blue to highlight the immature and mature forms of fibrin with red and blue, respectively. Given that erythrocyte deposition in the trabecular meshwork and erythrocyte accumulation in the aqueous chamber were considered to be typical alterations in the rat pup eyes examined in experiment 1, the severity of these alterations was graded in experiment 2, according to the following scheme: none, –; slight, +; moderate, 2+; and severe, 3+. The incidence of each grade in each group and sampling time was calculated.

Statistical analysis. The SAS system for Windows (release 8.2 TS2M0, SAS Institute, Cary, NC) was used for statistical analysis. The cumulative incidence of macroscopic and histopathologic findings was analyzed by using the one-tailed Fisher exact test. A P value less 0.05 was considered statistically significant.

Results

Experiment 1. ***Macroscopic findings in eyes and eye volume.*** Macroscopic evaluation of pups' physical condition including that of the eyes during the lactation period (PND 0 to 21) revealed no abnormalities in any of the strains. The day of eye opening was comparable among the 3 strains, and all pups' eyes opened between PND 13 and 16.

The incidences of macroscopic lesions identified in eyes during necropsy are summarized in Table 1. Ring-shaped red regions in the anterior ocular segment and red spots in the posterior ocular segment (Figure 1) occurred both unilaterally and bilaterally in both albino rat strains (WH and SpD); however, pups of the pigmented LE lacked such alterations. These alterations in WH and SpD rats were present during PND 8 through 19 and PND 3 through 14, respectively, and had disappeared by the end of the weaning stage (PND 21). The cumulative incidences of these ocular abnormalities were higher ($P < 0.05$) in WH than in SpD rats (Table 1).

Eye volume increased linearly in all 3 strains evaluated until approximately the time of eye opening, and the volume continued to increase slightly after this time point (Figure 2).

Microscopic findings of the eyeballs. The typical histologic features of ocular development in WH and LE rats are shown in Figure 3. There was little difference between these strains in the temporal changes of the basic histopathologic architecture of the eye during postnatal development, except for the hemorrhagic lesions. In WH rats, the fundamental structures of the ocular tissue were present at birth (PND 0; Figure 3 A). However, the ocular tissues, including iris, ciliary body, cornea, and lens, were premature in form, and the layered structure of nuclear cells was not discernable in any part of the retina. The aqueous chamber was not fully expanded and was filled with homogenous eosinophilic material, which was identified as mature fibrin (that is, blue) by

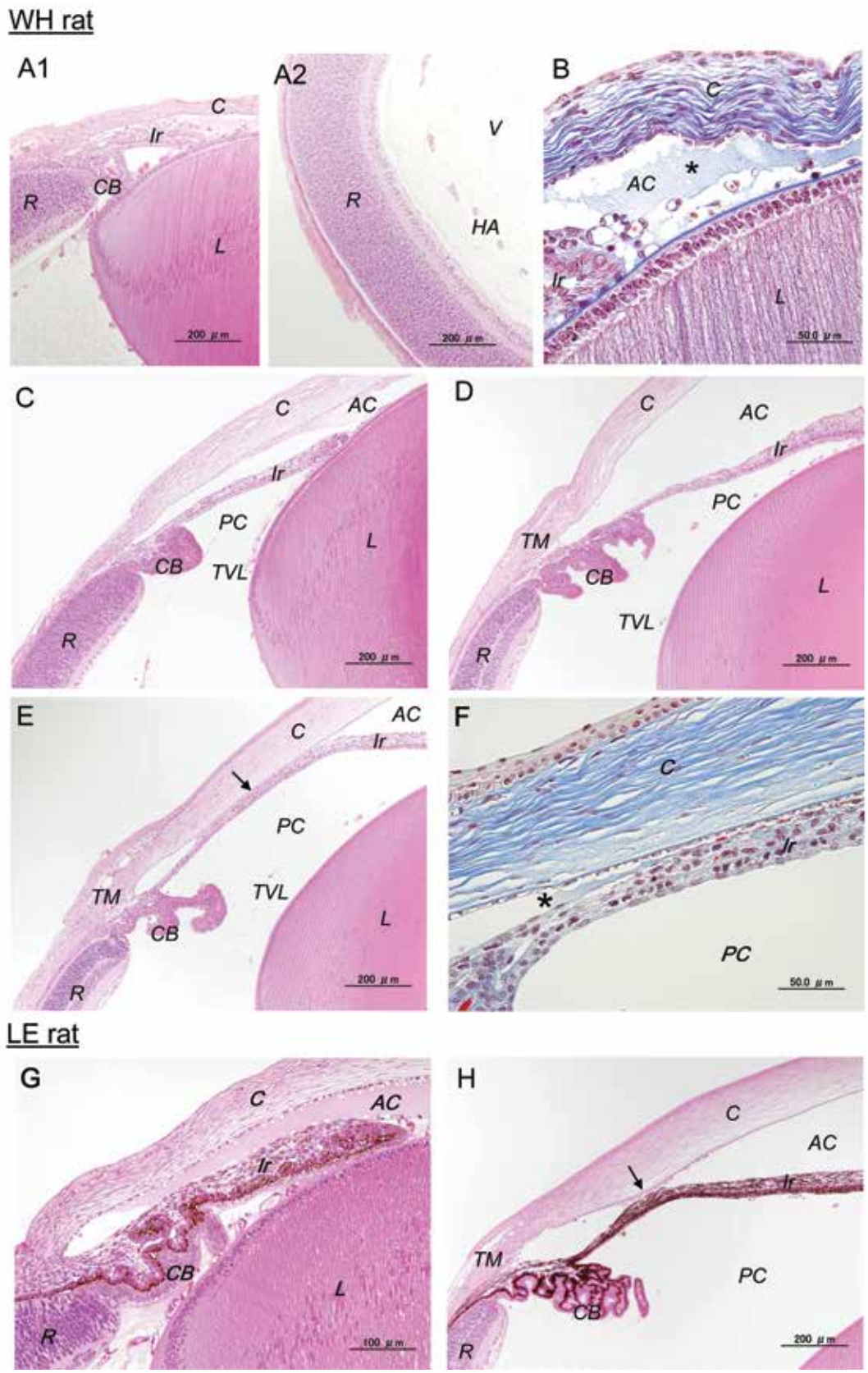

Figure 3. The development of ocular structures and various histopathologic findings in rat pups. Histopathologic micrographs of eyes from (A1, A2, B, C, D, E, and F) WH and (G and H) LE rats. (A1 and A2) PND 0. The fundamental structure of the ocular tissue is present. However, (A1) ocular tissues, such as the iris (*Ir*), ciliary body (*CB*), cornea (*C*), and lens (*L*) are in a premature form, and the aqueous chamber is not fully expanded. (A2) The

staining with Martius scarlet blue (Figure 3 B). At PND 6 through 8 (Figure 3 C), the iris was elongated, and spaces were present in both the anterior and posterior chambers. Separation of the neuroblastic layer into the outer and inner nuclear layers was noted in the posterior segment of retina. The principal ocular structures were completely formed and the iris was fully elongated by the time of eye opening (PND 13 through 16; Figure 3 D). The ciliary body was expanded, and the densities of both the tunica vasculosa lentis and hyaloid artery were decreased. The anterior end of the retina was mature and exhibited a fully layered structure. The aqueous chamber was expanded, and the formation of both the trabecular meshwork and Schlemm's canal in the chamber angle were confirmed. Partial iridocorneal adhesion (Figure 3 E) was present in some pups; in such cases, the iris was adhered to the cornea by mature fibrin (Figure 3 F). By PND 21, the eosinophilic material in the aqueous chamber had disappeared, and the iridocorneal adhesion was not visible; however, remnants of the tunica vasculosa lentis and hyaloid artery were present. Ocular development in LE pups was highly similar to that in WH rats, except for the addition of the pigment cell layers in the retina, ciliary body, and iris (Figure 3 G and H).

Erythrocyte deposition in the trabecular meshwork (Figure 4 A) and erythrocyte accumulation in the aqueous chamber (Figure 4 B) occurred in the anterior ocular segment of both the WH and SpD strains. These lesions corresponded to the ring-shaped red regions found at necropsy. In addition, small hemorrhagic foci were identified in the retina, choroid, and vitreous body in the posterior ocular segment (Figure 4 C through F), but their incidence was lower than that of the alterations depicted in Figure 4 A and B. These small foci may correspond to the red spots discernable on macroscopic examination. Retinal hemorrhage was present in the inner layer of the ganglionic optic nerve fibers (Figure 4 C) and nuclear layers (Figure 4 D), and vitreal hemorrhage occurred in areas around the hyaloid artery (Figure 4 E and F). These microscopic hemorrhagic lesions were present in some pups whose eyes appeared macroscopically normal at necropsy. The incidences of microscopic ocular lesions in pups are summarized in Table 2.

The deposition of erythrocytes in the trabecular meshwork occurred in all strains, and the cumulative incidence of the deposition was significantly ($P < 0.05$) higher in WH rats than in the other strains. Deposition of erythrocytes in the trabecular meshwork was detected in WH rats at PND 6 through 14, in SpD rats during PND 1 through 12, and in LE rats at PND 8 through 11 and had disappeared by approximately the time of eye opening.

Accumulation of erythrocytes in the aqueous chamber occurred only in the albino strains. In addition, the cumulative incidence of this erythrocyte accumulation was significantly ($P < 0.05$) higher in WH rats than in SpD rats. The accumulation of erythrocytes in the aqueous chamber in the WH and SpD rats was detected during PND 2 through 14 and PND 3 through 12, respectively, and had disappeared by approximately the time of the eye opening. However, phagocytosis of erythrocytes was not noted, even during the phase when these lesions disappeared.

Retinal hemorrhage occurred in both the WH and SpD strains. The cumulative incidence of this hemorrhage was significantly ($P < 0.05$) higher in WH rats than in SpD rats, although this hemorrhage occurred sporadically. Choroidal hemorrhage was present only in WH rats, and vitreal hemorrhage was noted in both the WH and LE strains. The incidences of these hemorrhages were very low, and they occurred sporadically.

Experiment 2. To identify the origin of the erythrocytes in the trabecular meshwork and aqueous chamber, we examined serial sections of representative eyes from WH rats at PND 7 through 14. Erythrocytes accumulated in areas near the tunica vasculosa lentis, a temporary vascular network (Figure 5); foci of erythrocytes did not occur near the iris, ciliary body, or chamber angle.

The incidences of macroscopic alterations and microscopic findings WH rats at PND 7 through 14 are summarized in Table 3. The incidence of the ring-shaped red regions in the anterior ocular segment peaked at PND 11 (50%) and gradually decreased thereafter. The incidence of red spots in the posterior ocular segment varied from 16% to 39% during the observation period, and there was no relevant peak in their occurrence. Histopathologic analysis of the eyes revealed that the deposition of erythrocytes in the trabecular meshwork and their accumulation in the aqueous chamber occurred throughout the observation period, and those incidences peaked during PND 9 through 12. The incidence of retinal hemorrhage was 6% to 31% throughout the observation period. Hemorrhage in the choroid and vitreous body occurred sporadically; however, there was no particular trend in the occurrence of hemorrhage during the observation period. Almost all litters had pups that demonstrated these macro- and microscopic alterations, and there was no apparent litter incidence bias in these ocular alterations.

Discussion

The present study confirmed the occurrence of intraocular hemorrhage in the pups of WH rats before eye opening. Ring-shaped red regions and red spots were present macroscopically at high incidence in the eyes of WH rats from PND 8 through 19. The cumulative incidence of these lesions reached 30% in experiment 1, and these alterations had disappeared by the end of the weaning stage (PND 21). Histopathologic analysis revealed that the ring-shaped red regions and red spots in the eyes could be attributed to hemorrhage of the tunica vasculosa lentis and of the retina, choroid, or hyaloid artery, respectively. These types of intraocular hemorrhage were present in both the WH and SpD strains, although the incidence was lower in SpD rats. Despite the lack of macroscopic alterations, deposition of erythrocytes in the trabecular meshwork, indicative of hemorrhage in the tunica vasculosa lentis, and hemorrhage in the hyaloid artery were present in LE rats. Therefore, intraocular hemorrhage may spontaneously occur in rats during normal ocular development regardless

nuclear layer structure is not recognizable in any part of the retina (*R*). (B) The aqueous chamber is filled with mature fibrin (*). A higher magnification view of the aqueous chamber is shown in panel A1. (C) PND 7. Elongation of the *Ir* is detected, and spaces are present in both the anterior chamber (*AC*) and posterior chamber (*PC*). (D) PND 14. The principal ocular structures are visible. The *Ir* is fully elongated, and the *CB* is expanded. (E) A partial iridocorneal adhesion (arrow) at PND 14. (F) A higher magnification view of an iridocorneal adhesion. The *Ir* was adhered to the *C* by mature fibrin (*). (G) PND 0, LE rat. The structure of the ocular tissue is visible, as shown in panel A1, except that pigment cell layers are present in the *R*, *CB* and *Ir*. (H) A partial iridocorneal adhesion (arrow) at PND 12. *HA*, hyaloid artery; *L*, lens; *TM*, trabecular meshwork; *TVL*, tunica vasculosa lentis; *V*, vitreous body. Hematoxylin and eosin (A1, A2, C, D, E, G, and H) and Martius scarlet blue (B and F) stains.

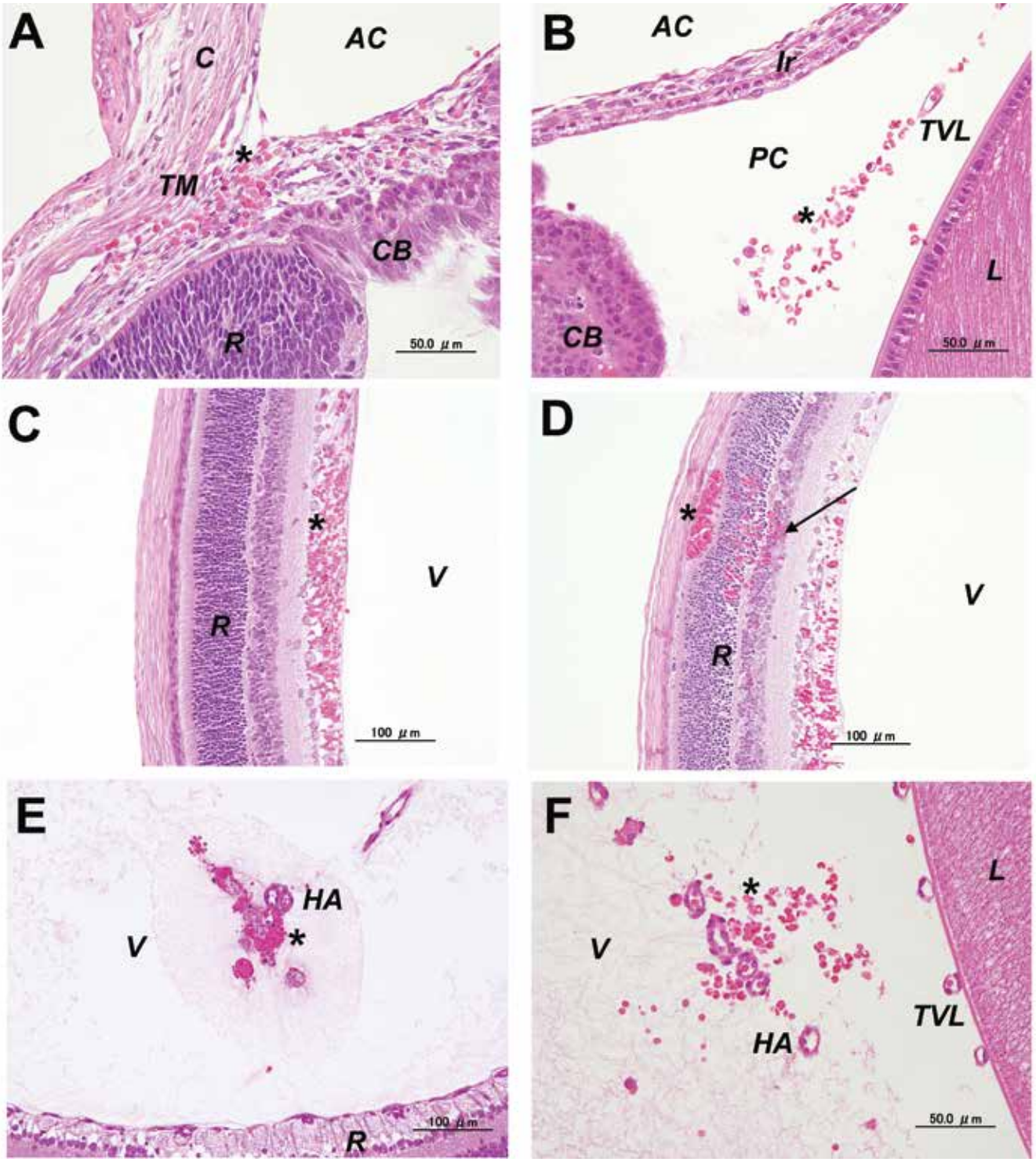

Figure 4. Histopathologic micrographs of intraocular hemorrhage located in the anterior and posterior ocular segments of (A through E) WH and (F) LE rat pups at PND 8 through 16. (A) Deposition of erythrocytes (*) in the trabecular meshwork (*TM*) at PND 10. (B) Accumulation of erythrocytes (*) in the posterior chamber (*PC*) at PND 10. (C) Hemorrhage (*) in the inner layer of the ganglionic optic nerve fibers of the retina (*R*) at PND 12. (D) Retinal hemorrhage (arrow) extends to the outer and inner nuclear layers of the *R* at PND 10. Choroidal hemorrhage (*) is present also. (E) Vitreal hemorrhage (*) surrounding the hyaloid artery (*HA*) is near the optic disk at PND 8. (F) Vitreal hemorrhage (*) around the *HA* is located posterior to the lens (*L*) at PND 16. *AC*, anterior chamber; *C*, cornea; *CB*, ciliary body; *Ir*, iris; *TVL*, tunica vasculosa lentis; *V*, vitreous body. Hematoxylin and eosin stain.

Table 2. The incidences of microscopic ocular lesions in the pups of 3 rat strains at PND 0-21

Strain	PND 0	1	2	3	4	5	6	7	8	9	10	11	12	13	14	15	16	17	18	19	20	21	Cumulative incidence
WH																							
Total no. of pups examined	2	3	3	3	2	3	3	3	3	3	2	2	2	2	2	2	2	3	3	2	2	2	54
No. of pups with any microscopic lesion	0	0	1	0	0	0	1	1	0	2	2	2	2	2	2	0	1	0	0	0	0	0	16 (29.6)[a]
No. of pups with erythrocyte deposition in the trabecular meshwork	0	0	0	0	0	0	1	1	0	2	2	2	2	2	2	0	0	0	0	0	0	0	14 (25.9)[c]
No. of pups with erythrocyte accumulation in the aqueous chamber	0	0	1	0	0	0	**1**	0	0	**1**	**2**	**2**	**1**	**1**	**1**	0	0	0	0	0	0	0	10 (18.5)[e]
No. of pups with retinal hemorrhage	0	0	0	0	0	0	0	0	0	0	**1**	0	**1**	**1**	0	0	1	0	0	0	0	0	4 (7.4)[g]
No. of pups with choroidal hemorrhage	0	0	0	0	0	0	0	0	0	0	**1**	0	0	0	0	0	*1*	0	0	0	0	0	2 (3.7)
No. of pups with vitreal hemorrhage	0	0	0	0	0	0	0	0	1	0	0	0	0	0	0	0	0	0	0	0	0	0	1 (1.9)
SpD																							
Total no. of pups examined	4	4	4	4	4	4	4	5	4	5	5	5	5	5	5	4	4	4	4	4	4	4	95
No. of pups with any microscopic lesion	0	1	0	1	0	0	0	1	0	4	2	1	1	1	0	0	0	0	0	0	0	0	12 (12.6)[b]
No. of pups with erythrocyte deposition in the trabecular meshwork	0	1	0	0	0	0	0	1	0	4	2	1	1	0	0	0	0	0	0	0	0	0	10 (10.5)[d]
No. of pups with erythrocyte accumulation in the aqueous chamber	0	0	0	1	0	0	0	0	0	**1**	0	0	**1**	0	0	0	0	0	0	0	0	0	3 (3.2)[f]
No. of pups with retinal hemorrhage	0	0	0	0	0	0	0	0	0	0	0	0	0	1	0	0	0	0	0	0	0	0	1 (1.1)
No. of pups with choroidal hemorrhage	0	0	0	0	0	0	0	0	0	0	0	0	0	0	0	0	0	0	0	0	0	0	0 (0.0)
No. of pups with vitreal hemorrhage	0	0	0	0	0	0	0	0	0	0	0	0	0	0	0	0	0	0	0	0	0	0	0 (0.0)
LE																							
Total no. of pups examined	4	4	4	4	4	4	4	4	3	4	4	4	4	4	4	4	4	4	4	4	4	4	87
No. of pups with any microscopic lesion	0	0	0	0	1	0	0	0	2	3	2	1	0	0	0	0	1	0	0	0	0	0	10 (11.5)[b]
No. of pups with erythrocyte deposition in the trabecular meshwork	0	0	0	0	0	0	0	0	2	3	2	1	0	0	0	0	0	0	0	0	0	0	8 (9.2)[d]
No. of pups with erythrocyte accumulation in the aqueous chamber	0	0	0	0	0	0	0	0	0	0	0	0	0	0	0	0	0	0	0	0	0	0	0 (0.0)[f]
No. of pups with retinal hemorrhage	0	0	0	0	0	0	0	0	0	0	0	0	0	0	0	0	0	0	0	0	0	0	0 (0.0)[h]
No. of pups with choroidal hemorrhage	0	0	0	0	0	0	0	0	0	0	0	0	0	0	0	0	0	0	0	0	0	0	0 (0.0)
No. of pups with vitreal hemorrhage	0	0	0	0	1	0	0	0	0	0	0	0	0	0	0	0	1	0	0	0	0	0	2 (2.3)

The values in parentheses indicate the cumulative incidence as a percentage. Bold type indicates simultaneous occurrence with deposition of erythrocytes in the trabecular meshwork; italics indicate simultaneous occurrence with retinal hemorrhage.

[a, b]These values differ significantly ($P < 0.05$, one-tailed Fisher exact test).

[c, d]These values differ significantly ($P < 0.05$, one-tailed Fisher exact test).

[e, f]These values differ significantly ($P < 0.05$, one-tailed Fisher exact test).

[g, h]These values differ significantly ($P < 0.05$, one-tailed Fisher exact test).

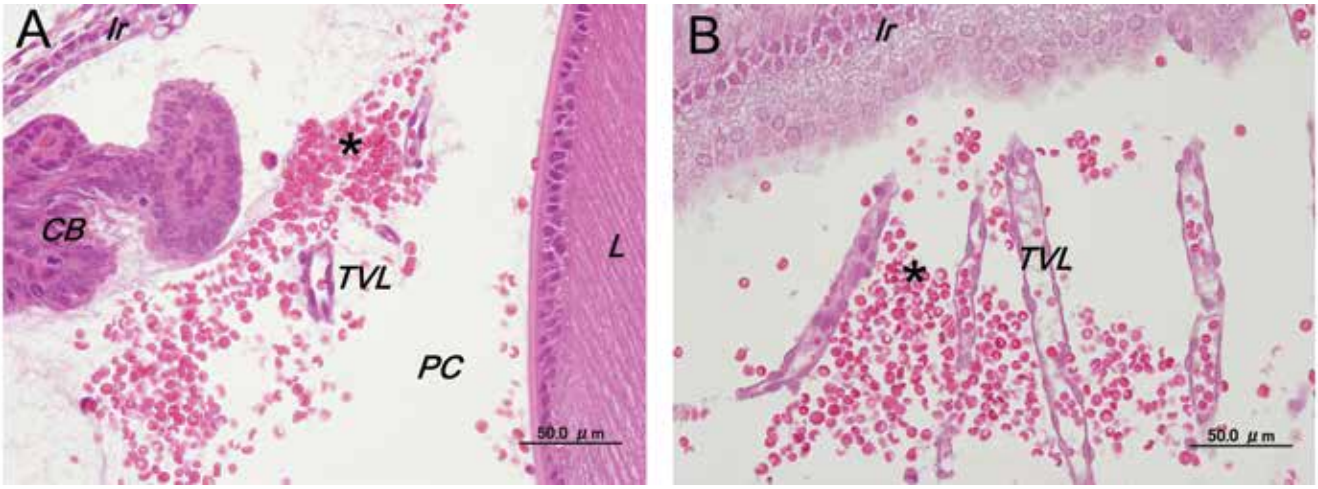

Figure 5. Histopathologic micrographs of hemorrhages in the posterior chamber of WH rat pups at PND 10. (A and B) Serial sections indicate a characteristic location for the hemorrhage, that is, the hemorrhagic focus (*) is restricted to the region of the tunica vasculosa lentis (*TVL*) and does not involve the iris (*Ir*) or ciliary body (*CB*). *L*, lens; *PC*, posterior chamber. Hematoxylin and eosin stain.

Table 3. Age-related changes in the incidences of macroscopic findings at necropsy and microscopic lesions in WH rats at PND 7–14

		PND							
		7	8	9	10	11	12	13	14
Total no. of litters examined		4	4	4	3	4	3	4	4
Total no. of pups examined		39	27	38	33	26	31	38	36
% of litters with pups with any macroscopic lesion		100.0	100.0	100.0	100.0	100.0	66.7	100.0	100.0
% of pups with any macroscopic lesion		33.3	63.0	52.6	60.6	65.4	45.2	47.4	27.8
% of pups with ring-shaped red region in the anterior ocular segment		12.8	37.0	39.5	45.5	50.0	35.5	13.2	2.8
% of pups with red spots in the posterior ocular segment		20.5	29.6	26.3	21.2	23.1	16.1	39.5	25.0
% of litters with pups with any microscopic lesion		100.0	100.0	100.0	100.0	100.0	100.0	100.0	100.0
% of pups with any microscopic lesion		64.1	33.3	55.3	57.6	80.8	64.5	50.0	50.0
% of pups with deposition of erythrocytes in the trabecular meshwork	Total	25.6	18.5	55.3	54.5	57.7	54.8	20.7	19.4
	+	10.3	7.4	28.9	9.1	34.6	25.8	17.2	19.4
	2+	7.7	7.4	15.8	18.2	19.2	29.0	3.4	0.0
	3+	7.7	3.7	10.5	27.2	3.8	0.0	0.0	0.0
% of pups with accumulation of erythrocytes in the aqueous chamber	Total	23.1	18.5	39.5	51.5	38.5	41.9	20.7	25.0
	+	7.7	0.0	21.1	15.2	30.8	29.0	13.8	22.2
	2+	7.7	11.1	13.2	18.2	7.7	12.9	6.9	2.8
	3+	7.7	7.4	5.3	18.2	0.0	0.0	0.0	0.0
% of pups with retinal hemorrhage		30.8	14.8	7.9	9.1	19.2	6.5	31.0	13.9
% of pups with choroidal hemorrhage		5.1	0.0	2.6	0.0	0.0	0.0	0.0	8.3
% of pups with vitreal hemorrhage		15.4	7.4	0.0	3.0	0.0	0.0	0.0	5.6

of the strain; however, the region, degree, and incidence of these alterations differ among strains. Our previous inability to note intraocular hemorrhages in SpD rats may reflect the timing of sampling for eye examination. According to the standard testing protocol for reproductive toxicity studies,[17] eye examinations usually are performed only after weaning, by which time the intraocular hemorrhages we describe here have disappeared. However, the reason underlying the lack of any literature describing macroscopic ocular alterations or intraocular hemorrhage in rat pups, especially SpD rats, which have long been used in toxicologic studies, remains unknown but may reflect the low incidence of intraocular hemorrhage in this strain.

Unlike humans, whose eyes are already open at birth, eye opening in rats occurred between PND 13 and 16 regardless of strain. The time course of ocular development in rats is considerably different from that in humans. In fact, in our microscopic examination, only the fundamental structure of the ocular tissues was in place at birth (PND 0). The principal structures were nearly complete by the time of eye opening (PND 13 to 16), after which ocular tissue maturation occurred (until PND 21). The

number of previous studies focusing on ocular development in rats is limited; however, a few reports describe histopathologic analysis of postnatal ocular development in rats. According to these reports, the time course of ocular development in rats after birth can be summarized as follows. In the retina, the prominent neuroblastic layer begins to separate into the outer and inner nuclear layers at PND 5, and the mature layered structure completes its formation at PND 14.[3] In the iris, the tissue matures at PND 10.[1,8] In the chamber angle, the trabecular meshwork and Schlemm's canal develop after PND 10.[14] In addition, the tunica vasculosa lentis and hyaloid vessels, which are structures within the temporary vascular network, regress within 3 wk after birth.[4,12] Our microscopic findings are highly consistent with these previous reports. In addition, the eye volume of rats increased linearly until eye opening and continued to increase slightly after this time point in the present study. These facts mirror the results of our histopathologic analysis of ocular development. It should be noted that the homogenous eosinophilic materials found in the aqueous chamber at birth were identified as mature fibrin, which gradually disappeared until weaning in all 3 strains. We could not locate any previous report regarding fibrin deposition in the aqueous chamber, and the physiologic role of such a deposition during ocular development is unknown. The deposited fibrin possibly maintains the space for the aqueous chamber during the primary development stage, given that fibrin can be degraded by fibrinolysis factors in the aqueous humor[2,16] during development. Overall, there are no interstrain differences with regard to overall ocular development in rats, with the exception of the pigmentation process in LE rats.

Our detailed analysis of serial sections of rat eyes indicated that the erythrocytes in the trabecular meshwork and aqueous chamber originated from hemorrhage in the tunica vasculosa lentis. The tunica vasculosa lentis is a structure consisting of a temporary vascular network and exhibits both growth and regression processes during ocular development. The regression of the temporal vascular network begins after birth and is completed within 3 wk.[12] In fact, we noted only a remnant of the tunica vasculosa lentis at PND 21 in our study. The mechanism underlying the regression of the temporal vascular network has been well studied.[10-12] This regression is initiated by macrophage-mediated apoptosis of vascular endothelial cells. Consequently, blood flow in these vessels is blocked, and a second phase of apoptosis begins in the remaining vascular endothelial cells. In addition, infusion of the blood component from the vessels into the aqueous chamber occurs during this process. Various colleagues[5] have used scanning electron microscopy to confirm the leakage of erythrocytes from the tunica vasculosa lentis at PND 5. The same finding was reported by other investigators,[13] who visualized the erythrocytes extruding through small holes in the capillary wall. Given these findings, we hypothesize that the blood vessels in the eyes of WH rats are more vulnerable than are those in the other strains, such that erythrocyte leakage is more likely to occur in WH rats than in other strains. The leaked erythrocytes may drain into the aqueous chamber and then into the trabecular meshwork through the flow of the aqueous humor. In adult rats, leaked erythrocytes perhaps are removed through trabecular meshwork; however, the trabecular meshwork and Schlemm's canal are immature before eye opening, thus leading to erythrocyte accumulation in the aqueous chamber and trabecular meshwork. After the maturation of the trabecular meshwork and Schlemm's canal, the erythrocytes would be removed, and the intraocular alterations therefore would disappear by the weaning stage. Hemorrhage in the tunica vasculosa lentis may be a physiologic process that is characteristic of ocular development in rats, and these alterations do not seem to affect ocular growth or visual function.

In contrast to hemorrhage in the tunica vasculosa lentis, there were no particular age-associated trends regarding the hemorrhage in the retina, choroid, and vitreous body. Whereas hemorrhagic alterations in the retina and vitreous body of rat pups have not previously been reported, spontaneous hemorrhage in these tissues has been reported to occur in adult rats.[7,13] One group[13] reported vitreal hemorrhage from a remnant hyaloid artery in Wistar rats at 7 wk old, and another[18] attributed the vitreal hemorrhage noted in the previously cited study[13] to regression of the hyaloid artery. The hyaloid artery in rats primarily regresses within 3 wk after birth.[4] We obtained similar results in our study, namely, vitreal hemorrhage occurred in the region near the hyaloid artery. Therefore, vitreal hemorrhage would occur during the regression of the hyaloid artery. Spontaneous hemorrhage in the retina has been reported to occur only in adult rats.[7] In addition, our results indicate that spontaneous hemorrhage of the retina occurs in rat pups, although whether the hemorrhage in the rat pups resulted from the same mechanism as that responsible for hemorrhage in adult rats is unknown. No published report concerning hemorrhage in the choroid in either pups or adult rats. The mechanism responsible for the hemorrhage observed in rat pups still needs to be elucidated.

In conclusion, the present study is perhaps the first report to describe the spontaneous intraocular hemorrhage that occurs during postnatal ocular development in rats. These hemorrhages occur during normal ocular development regardless of strain; however, the region, degree, and incidence of intraocular hemorrhages differ among strains, perhaps suggesting the involvement of genetic factors. The hemorrhages involve several ocular tissues, including the tunica vasculosa lentis, retina, choroid, and hyaloid artery. The hemorrhages in the tunica vasculosa lentis and hyaloid artery may result from the leakage of erythrocytes from the temporary vasculature of these tissues during regression, and the mechanisms underlying the hemorrhages in the retina and choroid remain to be elucidated.

Acknowledgments

We thank Ms Satoko Hirakawa and Ms Nobuko Tanaka (Research Center of Nihon Nohyaku) for providing excellent technical assistance.

References

1. **Berkow JW, Patz A.** 1964. Developmental histochemistry of the rat eye. Invest Ophthalmol **3:**22–33.
2. **Bernatchez SF, Tabatabay C, Deling D.** 1992. Urokinase-type plasminogen activator in human aqueous humor. Invest Ophthalmol Vis Sci **33:**2687–2692.
3. **Braekevelt CR, Hollenberg MJ.** 1970. The development of the retina of the albino rat. Am J Anat **127:**281–301.
4. **Cairns JE.** 1959. Normal development of the hyaloid and retinal vessels in the rat. Br J Ophthalmol **43:**385–393.
5. **Djano J, Griffin B, van Bruggen I, McMenamin PG.** 1999. Environmental scanning electron microscopic study of macrophages associated with the tunica vasculosa lentis in the developing rat eye. Br J Ophthalmol **83:**1384–1385.

6. **Fujiwara S, Matsui S, Hanabusa T, Maruyama T.** 1999. Fixative solution and sectioning method for eye. Jpn J Histotech **8:**13–18.
7. **Heywood R.** 1973. Some clinical observations on the eyes of Sprague–Dawley rats. Lab Anim **7:**19–27.
8. **Imaizumi M, Kuwabara T.** 1971. Development of the rat iris. Invest Ophthalmol **10:**733–744.
9. **King-Herbert A, Thayer K.** 2006. NTP workshop. Animal models for the NTP rodent cancer bioassay: stocks and strains—should we switch? Toxicol Pathol **34:**802–805.
10. **Lang R, Lustig M, Francols F, Sellinger M, Plesken H.** 1994. Apoptosis during macrophage-dependent ocular tissue remodeling. Development **120:**3395–3403.
11. **Latker CH, Kuwabara T.** 1981. Regression of the tunica vasculosa lentis in the postnatal rat. Invest Ophthalmol Vis Sci **21:**689–699.
12. **Meeson A, Palmer M, Calfon M, Lang R.** 1996. A relationship between apoptosis and flow during programmed capillary regression is revealed by vital analysis. Development **122:**3929–3938.
13. **Poulsom R, Marshall J.** 1985. Persistent hyaloid vasculature and vitreal haemorrhage in albino rats: a morphological and histological study. Exp Eye Res **40:**155–160.
14. **Remé C, Urner U, Acberhard B.** 1983. The development of the chamber angle in the rat eye. Morphological characteristics of developmental stages. Graefes Arch Clin Exp Ophthalmol **220:**139–153.
15. **The Act on Welfare and Management of Animals.** 1973. Act no. 105. Final amendment: 2011. Japan.
16. **Tripathi RC, Park JK, Tripathi BJ, Millard CB.** 1988. Tissue plasminogen activator in human aqueous humor and its possible therapeutic significance. Am J Ophthalmol **106:**719–722.
17. **US Environmental Protection Agency.** 1998. Health effect test guidelines OPPTS 870.3800. Reproduction and fertility effects. EPA 712-C-98-208.
18. **Williams D.** 2007. Rabbit and rodent ophthalmology. Eur J Companion Anim Pract **17:**242–252.